

the filtrate converted to TMS-oxime derivatives by the method above. The yields in Table I were obtained from the mass chromatograms using the TMS-oxime derivative of galactose, which was not a product, as an internal standard and are the average of six runs. In some runs, a GC peak corresponding in retention time to the TMS derivative of glucose was observed; no MS data were obtained.

Reaction of Arc Generated Carbon Vapor with D₂O. In a typical reaction, deuterium oxide (250 mmol) was reacted with carbon vapor using the method described above. GC/MS analysis of the TMS-oxime derivatives demonstrated that they contained the appropriate amount of deuterium and gave the yields in Table I which are the average of seven runs.

Reaction of Arc Generated Carbon Vapor with D₂O and Formaldehyde. In a typical reaction, deuterium oxide (250 mmol) and gaseous form-

aldehyde (27.6 mmol, from paraformaldehyde) were introduced separately into the reactor and condensed with carbon vapor. GC/MS analysis of the TMS-oxime derivatives demonstrated that the original carbohydrates contained both a CH₂O and a CD₂O and that the remaining carbons were deuterated (table). The yields in Table I are the average of four runs.

Acknowledgment. Support of this research by the National Science Foundation is gratefully acknowledged.

Supplementary Material Available: Retention times and mass spectral data for TMS-oxime derivatives of standard carbohydrates and those which are the products of the reactions described (9 pages). Order information is given on any current masthead.

Simple General Acid-Base Catalysis of Physiological Acetylcholinesterase Reactions

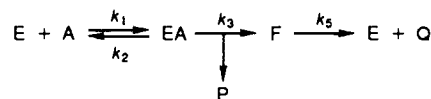
Alton N. Pryor,[†] Trevor Selwood,[†] Lee-Shan Leu,[†] Mark A. Andracki,[†] Bong Ho Lee,[†] Muralikrishna Rao,[†] Terrone Rosenberry,[‡] Bhupendra P. Doctor,[§] Israel Silman,^{||} and Daniel M. Quinn^{*†}

Contribution from the Department of Chemistry, The University of Iowa, Iowa City, Iowa 52242, Department of Pharmacology, Case Western Reserve University, Cleveland, Ohio 44106, Division of Biochemistry, Walter Reed Army Institute of Research, Washington, DC 20307, and Department of Neurobiology, Weizmann Institute of Science, Rehovot 76100, Israel. Received August 1, 1991

Abstract: Elements of transition-state stabilization by proton bridging have been characterized by measuring solvent isotope effects and proton inventories for hydrolyses of (acetylthio)choline (ATCh), (propionylthio)choline (PrTCh), and (butyrylthio)choline (BuTCh) catalyzed by acetylcholinesterases (AChEs) from *Electrophorus electricus*, fetal bovine serum, human erythrocytes, and *Torpedo californica*. For the *Electrophorus* enzyme, the acylation rate constant, $k_{\text{cat}}/K_m \{= (V/K)/[E]_T\}$, decreases in the order ATCh > PrTCh >> BuTCh. Solvent isotope effects for V/K of ATCh hydrolysis are usually within experimental error of unity, which is consistent with rate determination of the acylation stage of catalysis by a physical step, such as substrate diffusion. However, as substrate reactivity decreases the isotope effect increases, which indicates that the transition state of a chemical step is increasingly rate determining. A linear proton inventory for V/K of BuTCh hydrolysis indicates that this chemical transition state is stabilized by single proton transfer. Solvent isotope effects for V are ~2, and the corresponding proton inventories are invariably linear, irrespective of the source of AChE, the choice of substrate, the ionic strength of the medium, or the presence of the detergent TX100. The consistency of the results strongly suggests that AChE stabilizes chemical transition states of physiological reactions by one-proton, simple general acid-base catalysis. Therefore, elaborate themes in transition-state stabilization by proton transfer, such as multifunctional or charge-relay catalyses, do not appear to operate in the physiological functioning of AChE.

The physiological function of acetylcholinesterase (AChE¹) is the hydrolysis of the neurotransmitter acetylcholine (ACh) at nerve-nerve synapses and neuromuscular junctions.²⁻⁴ This reaction proceeds via an acylenzyme mechanism, outlined in Scheme I, that is similar to that of the serine proteases.⁵⁻⁸ Several observations in recent years have firmly entrenched this mechanism. Froede and Wilson trapped the acetyl-AChE intermediate formed during EE-AChE-catalyzed turnover of [³H]acetyl ACh and (acetylthio)choline (ATCh),⁹ thereby providing the first direct evidence for the acylenzyme mechanism. Their experiments showed that $V (= k_{\text{cat}}[E]_T)$ is 57-68% rate limited by the deacylation stage of the mechanism. Comparative sequences of cholinesterases^{10,11} and site-directed mutagenesis experiments¹⁰ indicate that S200 and H440 (TC-AChE numbering) are constituents of the active site. Perhaps the most significant report is that of the crystal structure of TC-AChE.¹² This structure shows that the active site sits at the bottom of a 15-Å depression

Scheme I



in the enzyme and contains the side chains of S200, H440, and E327 in a stereochemical relationship that is similar to that of

(1) Abbreviations: AChE, acetylcholinesterase; ATCh, (acetylthio)choline; BuTCh, (butyrylthio)choline; PrTCh, (propionylthio)choline; TCh, thiocholine; DTNB, 5,5'-dithiobis(2-nitrobenzoic acid); ONPA, *o*-nitrophenyl acetate; EE-AChE, *Electrophorus electricus* AChE; FBS-AChE, fetal bovine serum AChE; HE-AChE, human erythrocyte AChE; TC-AChE, *Torpedo californica* AChE; TX100, Triton X100; UDP, umbelliferyl diethyl phosphate; K , the Michaelis constant K_m ; V , the maximal velocity V_{max} ; V/K , V_{max}/K_m ; $D_2O V = V^{H_2O}/V^{D_2O}$, solvent isotope effect on V ; $D_2O K = K^{H_2O}/K^{D_2O}$, solvent isotope effect on K ; $D_2O V/K$, solvent isotope effect on V/K .

(2) Rosenberry, T. L. *Adv. Enzymol. Relat. Areas Mol. Biol.* **1975**, *43*, 103-218.

(3) Quinn, D. M. *Chem. Rev.* **1987**, *87*, 955-979.

(4) (a) Taylor, P. In *Pharmacological Basis of Therapeutics*; Gilman, A. G., Goodman, L. S., Murad, F., Eds.; MacMillan: New York, 1985; pp 110-129. (b) Froede, H. C.; Wilson, I. B. In *The Enzymes*, 3rd ed.; Boyer, P. D., Ed.; Academic: New York, 1971; Vol. 5, pp 87-114.

* Author to whom correspondence should be addressed.

[†] The University of Iowa.

[‡] Case Western Reserve University.

[§] Walter Reed Army Institute of Research.

^{||} Weizmann Institute of Science.

the S-H-D triad of the serine proteases.⁵⁻⁸

For the mechanism outlined in Scheme I, the steady-state kinetic parameters are given by the following equations:

$$V/K = k_{\text{cat}}[E]_{\text{T}}/K_{\text{m}} = \frac{k_1 k_3 [E]_{\text{T}}}{k_2 + k_3} \quad (1)$$

$$V = k_{\text{cat}}[E]_{\text{T}} = \frac{k_3 k_5 [E]_{\text{T}}}{k_3 + k_5} \quad (2)$$

These equations show that V/K is rate limited either by substrate binding (k_1) or by the chemical step(s) of acylation (k_3) and that V is rate limited by a combination of events in the acylation and deacylation stages of catalysis. The acylenzyme trapping experiment of Froede and Wilson⁹ described above necessitates that k_3 and k_5 contribute comparably to rate determination of V .

A hallmark of AChE catalysis is the tremendous catalytic power of the enzyme.^{3,13} The second-order rate constant, $k_{\text{cat}}/K_{\text{m}}$, for ACh and ATCh hydrolysis is $\sim 10^8 \text{ M}^{-1} \text{ s}^{-1}$ and is probably diffusion controlled.^{14,15} The turnover number, k_{cat} is $\sim 10^4 \text{ s}^{-1}$, 10^6 -fold faster than rate-determining turnover of acetyl-serine proteases¹⁶ and among the highest of enzymic turnover numbers. AChE accelerates the neutral hydrolysis of ACh by $\sim 10^{13}$ -fold,¹³ which corresponds to a transition-state stabilization of $\sim 18 \text{ kcal/mol}$. A proper accounting of the catalytic power of AChE requires enumeration and characterization of the interactions of the enzyme and the substrate-derived portion of the transition state. Among these is the set of general acid-base proton transfers that is amenable to probing by measurements of solvent isotope effects and proton inventories.¹⁷ Such experiments show that serine protease-catalyzed hydrolyses of extended peptide substrates involve transition states that are stabilized by multiple proton transfers,¹⁸⁻²⁴ consistent with charge-relay catalysis by the active

site S-H-D triad. Given the similarity alluded to above in the active site constituents of serine proteases and cholinesterases, one might expect indications from proton inventories of charge-relay catalysis (or some other mode of multifunctional catalysis). This paper describes experiments on hydrolyses of choline esters catalyzed by diverse AChEs that address these expectations.²⁵

Experimental Section

Materials. EE-AChE was purchased from Sigma Chemical Co. HE-AChE was purified from human red blood cells as described by Rosenberry and Scoggin.²⁶ FBS-AChE was purified from fetal bovine serum as described by De La Hoz et al.²⁷ TC-AChE was purified as described by Sussman et al.²⁸ The following reagents were used as received from the specified suppliers: ATCh chloride, BuTCh iodide, TX100, DTNB, $\text{NaH}_2\text{PO}_4 \cdot \text{H}_2\text{O}$, and $\text{Na}_2\text{HPO}_4 \cdot 7\text{H}_2\text{O}$ were purchased from Sigma. NaCl was purchased from EM Science, deuterium oxide (99.9% *d*) from Isotec Ltd., PrTCh iodide from Aldrich Chemical Co., and TCh iodide from K & K Laboratories. The water for buffer preparation was distilled and deionized by passage through a Barnstead mixed-bed ion-exchange column (Sybron Corp.).

Enzyme Kinetics and Data Treatment. AChE-catalyzed hydrolysis of thiocholine esters was monitored by following the production of thiocholine at 412 nm by the coupled continuous assay of Ellman et al.²⁹ Reactions were monitored on HP8452A, Beckman DU7, or Beckman DU40 UV-visible spectrophotometers. The kinetic parameters V and K were determined by nonlinear least-squares fitting³⁰ of $\{V_i, [A]\}$ data to the Michaelis-Menten equation, where V_i and $[A]$ are the initial velocity and substrate concentration, respectively:

$$V_i = \frac{V[A]}{K + [A]} \quad (3)$$

Values of k_{cat} and $k_{\text{cat}}/K_{\text{m}}$ were calculated by dividing V and V/K , respectively, by the enzyme concentration. A mass of 70 000 *pg* active site was used in the calculation of enzyme concentration.³ Initial velocities were measured by linear least-squares fitting of time courses for $\leq 5\%$ of total substrate turnover. The constituents of reaction media are specified in the footnotes of Table I and in the figure legends.

Thiocholine Inhibition. The mechanism of product inhibition by TCh was determined by measuring initial velocities of EE-AChE-catalyzed hydrolysis of ONPA at various fixed concentrations of TCh. Reactions were conducted at $25.0 \pm 0.1 \text{ }^\circ\text{C}$ in 0.1 M sodium phosphate buffer that contained 0.1 N NaCl, 1% MeCN (v/v), 16 pM AChE, $[\text{TCh}] = 0-1.85 \text{ mM}$, and $[\text{ONPA}]_0 = 0.125-4.0 \text{ mM}$. The dependence of the pseudo-first-order rate constant V/K on $[\text{TCh}]$ was determined under the same conditions, save that the reaction medium contained 62 pM AChE, $[\text{ONPA}]_0 = 0.04 \text{ mM}$, and no MeCN. Values of V/K were calculated by fitting time course data over >3 half-lives to a first-order kinetics function.

Solvent Isotope Effects and Proton Inventories. Solvent isotope effects were determined by measuring kinetic parameters in equivalently buffered H_2O and D_2O .¹⁷ The number and nature of transition-state proton bridges that contribute to the solvent isotope effect are characterized by the proton inventory technique,¹⁷ in which rates are measured in a series of buffered mixtures of H_2O and D_2O . The dependence of rate or rate constant on the atom fraction n of deuterium in $\text{H}_2\text{O}-\text{D}_2\text{O}$ mixtures is described by the Gross-Butler equation,¹⁷ which takes on the following form when reactant-state protons do not contribute to the isotope effect:

$$k_n = k_0 \prod_i (1 - n + n\phi_i^{\ddagger}) \quad (4)$$

Equation 4 describes a polynomial dependence of k_n , the rate in solvent

- (5) Stroud, R. M. *Sci. Am.* **1974**, *231*, 74-88.
 (6) Blow, D. M. *Acc. Chem. Res.* **1976**, *9*, 145-152.
 (7) Kraut, J. *Annu. Rev. Biochem.* **1977**, *46*, 331-358.
 (8) Polgar, L. In *Hydrolytic Enzymes*; Neuberger, A., Brocklehurst, K., Eds.; Elsevier: Amsterdam, 1987; pp 159-200.
 (9) Froede, H. C.; Wilson, I. B. *J. Biol. Chem.* **1984**, *259*, 11010-11013.
 (10) (a) Taylor, P.; Gibney, G.; Camp, S.; Maulet, Y.; Ekström, T. J.; Rachinsky, T. L.; Li, Y. In *Cholinesterases: Structure, Function, Mechanism, Genetics, and Cell Biology*; Massoulié, J., Bacou, F., Barnard, E., Chatonnet, A., Doctor, B. P., Quinn, D. M., Eds.; American Chemical Society: Washington, D.C., 1991; pp 179-185. (b) Gibney, G.; Camp, S.; Dionne, M.; MacPhee-Quigley, K.; Taylor, P. *Proc. Natl. Acad. Sci. U.S.A.* **1990**, *87*, 7546-7550.
 (11) Gentry, M. K.; Doctor, B. P. In *Cholinesterases: Structure, Function, Mechanism, Genetics, and Cell Biology*; Massoulié, J., Bacou, F., Barnard, E., Chatonnet, A., Doctor, B. P., Quinn, D. M., Eds.; American Chemical Society: Washington, D. C., 1991; pp 394-398.
 (12) Sussman, J. L.; Harel, M.; Frolow, F.; Oefner, C.; Goldman, A.; Tokar, L.; Silman, I. *Science* **1991**, *253*, 872-879.
 (13) Schowen, R. L. In *Transition States of Biochemical Processes*; Gandour, R. D., Schowen, R. L., Eds.; Plenum: New York, 1978; pp 77-114. Schowen estimated the rate constant for neutral hydrolysis of acetylcholine at $8 \times 10^{-10} \text{ s}^{-1}$, which is $\sim 10^{13}$ -fold slower than k_{cat} for the AChE-catalyzed reaction.
 (14) Bazelyansky, M.; Robey, E.; Kirsch, J. F. *Biochemistry* **1986**, *25*, 125-130.
 (15) Nolte, H.-J.; Rosenberry, T. L.; Neumann, E. *Biochemistry* **1980**, *19*, 3705-3711.
 (16) For example, the first-order rate constant for hydrolytic deacylation of acetylchymotrypsin is 0.01 s^{-1} : Dupaix, A.; Béchet, J.-J.; Roucou, C. *Biochemistry* **1973**, *12*, 2559-2566.
 (17) (a) Schowen, K. B. J. In *Transition States of Biochemical Processes*; Gandour, R. D., Schowen, R. L., Eds.; Plenum: New York, 1978; pp 225-283. (b) Schowen, K. B.; Schowen, R. L. *Methods Enzymol.* **1982**, *87*, 551-606. (c) Venkatasubban, K. S.; Schowen, R. L. *CRC Crit. Rev. Biochem.* **1985**, *17*, 1-44. (d) Quinn, D. M.; Sutton, L. D. In *Enzyme Mechanisms from Isotope Effects*; Cook, P. F., Ed.; CRC Press: Boca Raton, FL, 1991; pp 73-126.
 (18) Hunkapiller, M. W.; Forgac, M. D.; Richards, J. H. *Biochemistry* **1976**, *15*, 5581-5588.
 (19) Elrod, J. P.; Hogg, J. L.; Quinn, D. M.; Venkatasubban, K. S.; Schowen, R. L. *J. Am. Chem. Soc.* **1980**, *102*, 3917-3922.
 (20) Stein, R. L.; Elrod, J. P.; Schowen, R. L. *J. Am. Chem. Soc.* **1983**, *105*, 2446-2452.
 (21) Stein, R. L. *J. Am. Chem. Soc.* **1983**, *105*, 5111-5116.
 (22) Stein, R. L. *J. Am. Chem. Soc.* **1985**, *107*, 5767-5775.

- (23) Stein, R. L.; Strimpler, A. M. *J. Am. Chem. Soc.* **1987**, *109*, 4387-4390.

- (24) Stein, R. L.; Strimpler, A. M.; Hori, H.; Powers, J. C. *Biochemistry* **1987**, *26*, 1305-1314.

- (25) A preliminary account of some of the results described in this paper was presented at the Third International Meeting on Cholinesterases in La Grande-Motte, France, May 12-16, 1990. Quinn, D. M.; Pryor, A. N.; Selwood, T.; Lee, B.-H.; Acheson, S. A.; Barlow, P. N. In *Cholinesterases: Structure, Function, Mechanism, Genetics, and Cell Biology*; Massoulié, J., Bacou, F., Barnard, E., Chatonnet, A., Doctor, B. P., Quinn, D. M., Eds.; American Chemical Society: Washington, D.C., 1991; pp 252-257.

- (26) Rosenberry, T. L.; Scoggin, D. M. *J. Biol. Chem.* **1984**, *259*, 5643-5652.

- (27) De La Hoz, D.; Doctor, B. P.; Ralston, J. S.; Rush, R. S.; Wolfe, A. D. *Life Sci.* **1986**, *39*, 195-199.

- (28) Sussman, J. L.; Harel, M.; Frolow, F.; Varon, L.; Tokar, L.; Futerman, A. H.; Silman, I. *J. Mol. Biol.* **1988**, *203*, 821-823.

- (29) Ellman, G. L.; Courtney, K. D.; Andres, V., Jr.; Featherstone, R. M. *Biochem. Pharmacol.* **1961**, *7*, 88-95.

- (30) Wentworth, W. E. *J. Chem. Educ.* **1965**, *42*, 96-103.

Table I. Kinetic Constants and Solvent Isotope Effects for AChE-Catalyzed Hydrolyses of Thiocholine Esters

enzyme	substrate	k_{cat} (s^{-1})	$10^{-5} k_{cat}/K_m$ ($M^{-1} s^{-1}$)	D_2O/V	$D_2O V/K$
EE-AChE	ATCh ^a	8800 ± 200	770 ± 60	2.15 ± 0.07	1.1 ± 0.1
	PrTCh ^b	3660 ± 70	250 ± 20	1.98 ± 0.08	1.7 ± 0.2
	BuTCh ^a	95 ± 3	0.80 ± 0.07	1.76 ± 0.09	1.87 ± 0.02
FBS-AChE	ATCh ^c	3640 ± 90	310 ± 20	2.30 ± 0.08	0.9 ± 0.1
HE-AChE	ATCh ^a	8200 ± 100	580 ± 20	2.02 ± 0.05	1.16 ± 0.08
TC-AChE	ATCh ^d	4280 ± 60	680 ± 40	2.15 ± 0.05	0.9 ± 0.1
	ATCh ^e	7600 ± 100	1100 ± 50	2.10 ± 0.07	
	ATCh ^f	2060 ± 30	960 ± 60	2.04 ± 0.05	

^a Reaction conditions: 25.0 ± 0.1 °C, 0.1 M sodium phosphate buffer, pH 7.26 or pD 7.79, 0.1 N NaCl, 0.3 mM DTNB, and 0.29 nM AChE (with ATCh) or 21 nM AChE (with BuTCh). ^b Reaction conditions: 24.80 ± 0.06 °C, 0.1 M sodium phosphate buffer, pH 7.46 or pD 8.02, 0.04 N NaCl, 1.2 mM DTNB, and 80 pM AChE. ^c Same conditions as in footnote a, save that reactions were run at pH 7.24 or pD 7.88 and contained 75 pM AChE. ^d Reaction conditions: 25.3 ± 0.1 °C, 0.1 M sodium phosphate buffer, pH 7.44 or pD 8.04, 0.1 N NaCl, 1.2 mM DTNB, and 20 pM AChE. ^e Reaction conditions: 25.22 ± 0.07 °C, 0.1 M sodium phosphate buffer, pH 7.46 or pD 8.02, 0.04 N NaCl, 1 mM TX100, 1 mM DTNB, and 84 pM AChE. ^f Reaction conditions: 25.31 ± 0.06 °C, 10 mM sodium phosphate buffer, pH 7.72 or pD 8.36, 10 mM NaCl, 1 mM DTNB, and 40 pM AChE.

isotopic mixtures, on k_0 , the rate in H_2O , and on a product of terms that contain transition-state fractionation factors ϕ^T for each of x protons that contribute to the isotope effect. When the isotope effect arises from a single proton transfer, a linear dependence of k_n on n results, whereas multiple proton transfers produce nonlinear dependences on n . Two methods are used to distinguish between these possibilities. First, polynomial regression analysis and attendant statistical analysis were used to determine the significance of higher order (i.e., quadratic, cubic, etc.) descriptions of proton inventories.^{17a,31} Second, proton inventories were fit by nonlinear least-squares procedures³⁰ to the quadratic version of eq 4:

$$k_n = k_0(1 - n + n\phi_1^T)(1 - n + n\phi_2^T) \quad (5)$$

If the solvent isotope effect arises from a single proton transfer, one of the ϕ values determined by fitting data to eq 5 will be close to or within error of unity.

Active Site Titration of EE-AChE. A commercial preparation of EE-AChE was used for some of the experiments described herein. Therefore, the active site concentration of samples of the enzyme was determined by titration with umbelliferyl diethyl phosphate (UDP). Synthesis of UDP and its characterization as an AChE inhibitor are described elsewhere.³² Release of umbelliferone on interaction of UDP with EE-AChE was monitored by fluorescence spectroscopy on an SLM-Aminco SPF500C fluorimeter. Fluorescence emission was measured at 456 nm on excitation at 326 nm. Reactions were conducted at 25.0 ± 0.2 °C in a 0.1 M sodium phosphate buffer, pH 7.3, that contained 0.1 N NaCl and 1 μ M UDP. A calibration plot of fluorescence emission versus umbelliferone concentration was linear, with a slope of $(4.72 \pm 0.07) \times 10^7 M^{-1}$ and an intercept of 0.23 ± 0.05 . The background fluorescence (F_b) of the titration solution before addition of AChE was 0.699. This reading corresponds to that from 9.9 nM umbelliferone, and thus the titrant UDP contains a <1% contaminant of its hydrolytic product. The time course of fluorescence emission increase following addition of AChE to the titration solution was fit to the following first-order equation:³⁰

$$F = (F_0 - F_{inf})e^{-kt} + F_{inf} \quad (6)$$

F , F_0 , and F_{inf} are the emission intensities at times t , 0, and infinity, respectively; k is the first-order rate constant. The enzyme concentration was calculated from the value of $F_{inf} - F_b$ using the parameters of the calibration plot.

Results

Figure 1 shows the time course for fluorescence increase on interaction of UDP with EE-AChE. Least-squares analysis of the data gives $k = (8.7 \pm 0.3) \times 10^{-3} s^{-1}$, which on division by the concentration of UDP gives a second-order rate constant of $8700 \pm 300 M^{-1} s^{-1}$. The enzyme concentration, calculated as described in the Experimental Section, is 8.6% of that expected on the basis of protein mass. A duplicate experiment (not shown) gave an active site concentration that was 10% of the expected value. The average of these values, 9.3%, was used to calculate

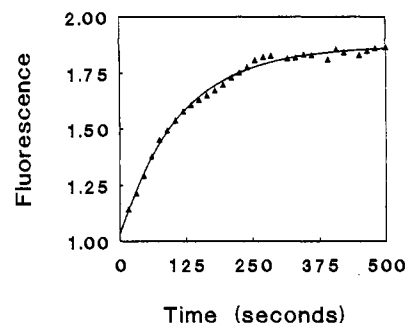


Figure 1. Fluorescence titration of the active site of EE-AChE with umbelliferyl diethyl phosphate (UDP). Reaction conditions are specified in the Experimental Section. The curved line is a nonlinear least-squares fit to eq 6.

the concentration of EE-AChE samples for experiments described in this paper.

Similar active site titrations of the AChE preparations from fetal bovine serum and *T. californica* were conducted. The titrations gave active site concentrations³² that are 100% of those expected from protein mass, within experimental error. Therefore, these AChE preparations are highly pure.

Solvent isotope effects on V and V/K were determined as described in the Experimental Section for choline ester hydrolyses catalyzed by four AChEs, and the results are summarized in Table I. $D_2O V/K$ values are usually ~ 1 for AChE-catalyzed hydrolysis of ATCh, which is consistent with diffusional rate limitation.^{14,15} The contribution of chemical steps to rate determination of V/K can be increased by utilizing less reactive substrates. Hence, it is not surprising that $D_2O V/K$ increases as k_{cat}/K_m decreases (compare ATCh to PrTCh and to BuTCh in Table I).

On the other hand, $D_2O V$ values are ~ 2 , which suggest rate limitation by the transition state of a chemical step. Proton inventories for V of all of the reactions listed in Table I are linear, such as that for the TC-AChE-catalyzed hydrolysis of ATCh shown in Figure 2. The figure also shows a linear proton inventory for V/K of EE-AChE-catalyzed hydrolysis of BuTCh. No other proton inventories of V/K are reported herein. Polynomial regression analyses^{17a,31} of all proton inventories showed that the quadratic terms were not significant at the 80% confidence level. In addition, nonlinear least-squares fitting³⁰ of proton inventories to eq 5 showed that for each reaction a single fractionation factor accounts for >80% of the solvent isotope effect. Therefore, on statistical grounds, linear descriptions only of proton inventories are justified. The plots of Figure 2 provide visual confirmation of the indicated one-proton origin of solvent isotope effects for AChE-catalyzed hydrolyses of thiocholine esters.

AChE-catalyzed hydrolysis of ATCh is complicated by substrate inhibition, as shown in Figure 3 for reactions in H_2O and D_2O . Substrate inhibition is thought to arise when a second substrate molecule binds to and prevents the turnover of the acylenzyme intermediate.³³ For this inhibition mechanism, the

(31) Polynomial regression analyses were performed with the computer program MYSTAT, available from SYSTAT, 1800 Sherman Avenue, Evanston, IL 60201.

(32) Schlom, P. S.; Gillespie, S.; Selwood, T.; Knuth, T. M.; Quinn, D. M. *Arch. Biochem. Biophys.*, submitted for publication.

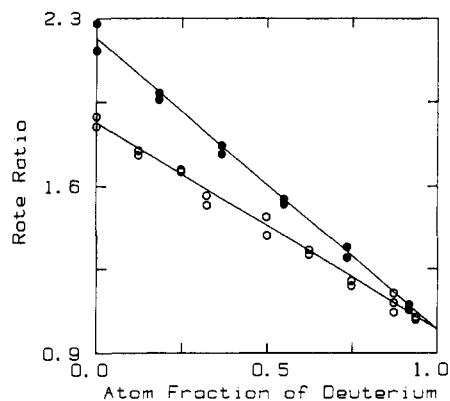


Figure 2. Proton inventories for AChE-catalyzed hydrolyses of choline esters. Linear fits are displayed, and rates or rate constants are divided by the least-squares extrapolated value in D_2O (i.e., $n = 1$), so that ratios are plotted on the y axis. Proton inventory of V for TC-AChE-catalyzed hydrolysis of ATCh (●). Initial rates were measured at 25.51 ± 0.07 °C in a 0.1 M sodium phosphate buffer, pH 7.44 and equivalent pL in H_2O - D_2O mixtures, that contained 0.1 N NaCl, 1.06 mM ATCh (= $16K$), 0.94 mM DTNB, and 40 pM TC-AChE. A nonlinear least-squares fit of the proton inventory to eq 5 gave $\phi_1^T = 0.48 \pm 0.06$ and $\phi_2^T = 0.95 \pm 0.10$. Thus, 90% of the observed solvent isotope effect of 2.2 arises from a single proton transfer. Proton inventory of V/K for EE-AChE-catalyzed hydrolysis of BuTCh (○). First-order rate constants were determined at 25.00 ± 0.05 °C in a 0.1 M sodium phosphate buffer, pH 7.26 and equivalent pL, that contained 0.1 N NaCl, $[BuTCh]_0 = 0.075$ mM (= $K/16$), $[DTNB]_0 = 0.2$ mM, and 59 nM AChE. A nonlinear least-squares fit of the proton inventory to eq 5 gave $\phi_1^T = 0.58 \pm 0.08$ and $\phi_2^T = 0.93 \pm 0.12$. Thus, 83% of the observed isotope effect of 1.87 comes from a single proton transfer.

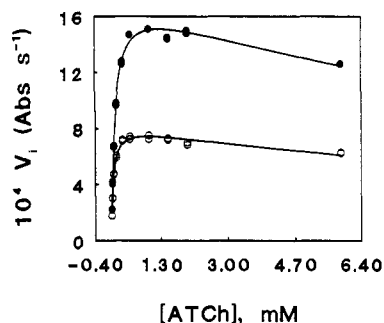


Figure 3. Substrate inhibition by ATCh of EE-AChE. Initial velocities were determined at 25.0 ± 0.1 °C in a 0.1 M sodium phosphate buffer, pH 7.3 or pD 7.8, that contained 0.1 N NaCl, 0.6 mM DTNB, and 0.21 nM AChE. The curved lines are nonlinear least-squares fits to eq 7, as described in the Results section.

dependence of initial velocity on substrate concentration is given by eq 7, in which K_{Ai} is the substrate-acylenzyme dissociation constant:

$$V_i = \frac{V[A]}{K + [A](1 + [A]/K_{Ai})} \quad (7)$$

Nonlinear least-squares³⁰ fitting of the plots in Figure 3 to this equation gave the following results: ${}^{D_2}V = 2.14 \pm 0.05$; $K^{H_2O} = 0.107 \pm 0.005$ mM, $K^{D_2O} = 0.052 \pm 0.003$ mM. Therefore, ${}^{D_2}K = 2.0 \pm 0.1$ and ${}^{D_2}V/K = 1.05 \pm 0.08$. $K_{Ai}^{H_2O} = 15 \pm 1$ mM and $K_{Ai}^{D_2O} = 17 \pm 2$ mM; therefore, ${}^{D_2}K_{Ai} = 0.9 \pm 0.1$. The solvent isotope effects for V and V/K are the same as those determined from fitting data to the Michaelis-Menten equation for $[ATCh]_0 \leq 0.5$ mM (cf. Table I). The lack of a palpable isotope effect on K_{Ai} suggests that ligand binding to AChE, including substrate binding, is not solvent isotope sensitive. Moreover, proton inventories determined at $[ATCh]_0 = 10K$ and $20K$ were both linear (plots not shown). Similar results are obtained for HE-AChE-catalyzed hydrolysis of ATCh at $[ATCh]_0$

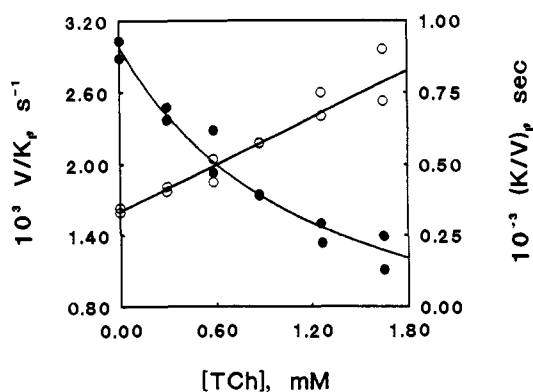


Figure 4. Linear noncompetitive inhibition of EE-AChE-catalyzed hydrolysis of ONPA by TCh. Least-squares fit of V/K_i versus $[TCh]$ data to eq 8 of the Results section (●, left y axis). Data are plotted according to the reciprocal transform of eq 8 (○, right y axis). Reaction conditions are specified in the Experimental Section.

= $8K$ and $21K$. Since the shape of the proton inventory does not change at increasing values of $[ATCh]_0 \gg K$, substrate inhibition does not affect the shape of the proton inventory.

Fits of $\{V_i, [A]\}$ data to eq 3 for EE-AChE-catalyzed hydrolysis of ONPA showed that, as TCh concentration increased, the Michaelis constant did not change (i.e., $K = 0.31 \pm 0.03$ mM), but V systematically decreased (data not shown). A replot of V^{-1} versus $[I]$ is linear; therefore, TCh is a linear noncompetitive inhibitor of EE-AChE. MeCN was used for dissolving and injecting the substrate ONPA; thus, the initial velocity measurements contained 1% MeCN (v/v). Because MeCN may affect the value of the inhibition constant K_i , the dependence of V/K on $[TCh]$ was determined under the same conditions as the initial velocity measurements but in the absence of MeCN (cf. the Experimental Section). For linear noncompetitive inhibition, V/K varies with $[TCh]$ according to eq 8:

$$V/K_i = \frac{V/K}{1 + [I]/K_i} \quad (8)$$

Figure 4 shows a nonlinear least-squares fit³⁰ of data to eq 8, from which $K_i = 1.23 \pm 0.05$ mM was calculated. The figure also shows that the corresponding double reciprocal transform is linear, as predicted by eq 8 and as expected for linear noncompetitive inhibition of EE-AChE by TCh.

Discussion

That the mechanism of AChE-catalyzed turnover of ATCh is a mimic of physiological hydrolysis of ACh is supported by numerous observations. For example, pH-rate profiles for the two substrates give similar estimates of enzyme pK_a values of 6.2–5.6.^{2,34,35} Values of k_{cat} and k_{cat}/K_m for ATCh and ACh are nearly identical, as are the fractions of rate determination of k_{cat} by the deacylation step k_5 .⁹

The proton inventories for V of various AChE-catalyzed hydrolyses of ATCh are invariably linear and therefore are consistent with single transition-state proton transfers that generate isotope effects of ~ 2 . Variation of substrate reactivity (ATCh versus PrTCh and BuTCh) has no effect on the shape of the proton inventory. The proton inventory for V of TC-AChE-catalyzed hydrolysis of ATCh remains linear when the ionic strength of the medium is decreased from 0.36 to 0.03 and when TX100 micelles are added to the reaction. Like the serine proteases,⁵⁻⁸ AChE may possess an oxyanion hole, comprised of the peptide NH groups of G118, G119, and A201,¹² that stabilizes oxyanionic transition states and tetrahedral intermediates by H-bonding. Linear proton inventories for AChE-catalyzed hydrolyses of choline esters suggest that H-bonding in this putative oxyanion hole does not give rise to ϕ^T values < 1 and thus to contributions to the solvent isotope

(34) (a) Krupka, R. M. *Biochemistry* 1966, 5, 1983–1988. (b) Krupka, R. M. *Biochemistry* 1966, 5, 1988–1998.

(35) Rosenberry, T. L. *Proc. Natl. Acad. Sci. U.S.A.* 1975, 72, 3834–3838.

(33) Wilson, I. B.; Cabib, E. *J. Am. Chem. Soc.* 1956, 78, 202–207.

effect. If such were the case, the multiprotonic origin of the solvent isotope effect would produce proton inventories that are nonlinear and downward bulging.

Two previous reports have described linear proton inventories for V of AChE-catalyzed hydrolysis of aryl esters, which include phenyl acetate³⁶ and *o*-nitrophenyl acetate.³⁷ Since k_{cat} values for these aryl esters are comparable to those for the acyl-similar choline esters ACh and ATCh,^{2,3} the results reported herein tend to corroborate the earlier reports. An important difference between aryl ester and choline ester substrates must be considered, however. The microscopic rate constants k_3 and k_5 can be calculated from k_{cat} and the fractions of rate determination by acylation, $f_a = k_3/(k_3 + k_5)$, and deacylation, $f_d = k_5/(k_3 + k_5)$, by using the following equations:

$$k_3 = k_{\text{cat}}/f_a \quad (9)$$

$$k_5 = k_{\text{cat}}/f_d \quad (10)$$

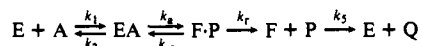
For EE-ATCh-catalyzed hydrolysis of ATCh, Froede and Wilson⁹ reported $k_{\text{cat}} = 8833 \text{ s}^{-1}$, in excellent agreement with the value in Table I, and $f_d = 0.57$; thus from eqs 9 and 10, $k_3 = 2.05 \times 10^4 \text{ s}^{-1}$ and $k_5 = 1.55 \times 10^4 \text{ s}^{-1}$. These rate constants can be compared to that for release of the product thiocholine (TCh) from the acetylenzyme intermediate as follows. TCh is a linear non-competitive inhibitor of EE-AChE-catalyzed hydrolysis of ONPA, with an inhibition dissociation constant $K_i = 1.23 \text{ mM}$. If the rate constant for binding of TCh to the acetylenzyme is comparable to that for ATCh binding to the free enzyme¹⁵ (i.e., $k_1 = k_{\text{cat}}/K_m = 7.7 \times 10^7 \text{ M}^{-1} \text{ s}^{-1}$; cf. Table I), then the TCh release rate constant is $k_R = 9.4 \times 10^4 \text{ s}^{-1}$. Because this value is comparable to k_3 and k_5 calculated above, k_{cat} of ATCh turnover is partially rate limited by release of the first product, TCh.³⁸ This situation does not occur in turnover of aryl esters, and therefore aryl ester proton inventories do not necessarily reflect the subtleties of the proton-transfer mechanism of AChE-catalyzed hydrolysis of choline esters. However, since the proton inventories for V of four AChE-catalyzed hydrolyses of ATCh are linear, it seems likely that transition states of physiological AChE reactions, like those of aryl ester turnover, are stabilized by simple general acid-base, one-proton catalysis.

The balance between contributions to rate determination from acylation and deacylation offers an additional complication in interpreting linear proton inventories for ATCh hydrolysis. In this case, the appropriate form of the Gross-Butler equation is given by the following:

(36) Kovach, I. M.; Larson, M.; Schowen, R. L. *J. Am. Chem. Soc.* **1986**, *108*, 3054-3056.

(37) Acheson, S. A.; Dedopoulou, D.; Quinn, D. M. *J. Am. Chem. Soc.* **1987**, *109*, 239-245.

(38) The following mechanism is an expansion of Scheme I that incorporates a kinetically significant product release step k_r :



Release of TCh terminates the acylation stage of catalysis, so that the acylation rate constant k_3 in eqs 1 and 2 becomes the following:

$$k_3 = \frac{k_R k_a}{k_R + k_a}, \quad \text{where } k_R = \frac{k_a k_r}{k_a + k_a}$$

Therefore, product release (k_R) is a component of k_3 . Since $k_3 = 2.05 \times 10^4 \text{ s}^{-1}$ and $k_R = 9.4 \times 10^4 \text{ s}^{-1}$, $k_a = 2.6 \times 10^4 \text{ s}^{-1}$. From these rate constants, one calculates that the chemical step k_a and the product release step k_r contribute 78% and 22%, respectively, to acylation rate determination.

$$V_0/V_n = \frac{f_a}{\prod_i (1 - n + n\phi_{di}^T)} + \frac{f_d}{\prod_j (1 - n + n\phi_{dj}^T)} \quad (11)$$

If both the acylation and deacylation transition states are stabilized by one-proton catalysis (i.e., $i = j = 1$) and the solvent isotope effects for acylation and deacylation are comparable (i.e., $\phi_a^T \approx \phi_d^T$), then eq 11 reduces to a linear dependence of V_n on n . This interpretation is most likely the correct one, since we observe linear proton inventories for V of ATCh hydrolysis catalyzed by AChEs from four disparate sources and since the proton inventories for both V and V/K (which contains rate constants for acylation only; cf. eq 1) of BuTCh hydrolysis are linear. On the other hand, if only deacylation (for example) is subject to an isotope effect, eq 11 reduces to the following:

$$V_0/V_n = f_a + \frac{f_d}{\prod_j (1 - n + n\phi_{dj}^T)} \quad (12)$$

This equation predicts an upward-bulging dependence of V_n on n if a single proton contributes to the solvent isotope effect (i.e., $j = 1$). However, if multiple protons contribute to the solvent isotope effect (i.e., $j > 1$), which normally produces a downward-bulging proton inventory, the effects can cancel to produce a fortuitously linear proton inventory. In such a case, a cryptic multiproton mechanism would be masked by the matched internal thermodynamics of AChE function.³ Again, the consistent observation of linear proton inventories for reactions of three choline substrates of widely ranging reactivity, catalyzed by four enzymes under various reaction conditions, augurs against a cryptic multiproton mechanism.

The observation of a single-proton mechanism for AChE-catalyzed hydrolyses of choline esters is surprising. Should this model withstand further scrutiny, a role other than proton-transfer (charge-relay) catalysis would be indicated for E327. For example, E327 may stabilize the H440 tautomer required for general acid-base function and/or electrostatically stabilize the incipient H440 imidazolium cation during catalysis. Such roles have been suggested for the aspartate constituent of the catalytic triads of serine proteases.⁸

The results described herein show that AChEs from disparate sources utilize catalytic mechanisms and modes of transition-state stabilization that are essentially the same. Acheson and Quinn³⁹ came to a similar conclusion for anilide and aryl ester hydrolyses catalyzed by EE-AChE and HE-AChE. Therefore, conservation of enzyme structure among the AChEs is reflected in conservation of reaction dynamics, and hence catalytic function, of the enzymes.

Acknowledgment. We thank Lilly Toker for skillful preparation of *Torpedo* AChE and John Stein for purification of human erythrocyte AChE. Support of this work was received from NIH Grants NS21334 to D.M.Q. and NS16577 to T.R., from a Revson Foundation grant to I.S., and from U. S. Army Medical Research and Development Command Contract No. DAMD17-89-C-9063 to I.S.

Registry No. AChE, 9000-81-1; ATCh chloride, 6050-81-3; PrTCh iodide, 1866-73-5; BuTCh iodide, 1866-16-6; TCh iodide, 7161-73-1; D₂, 7782-39-0.

(39) Acheson, S. A.; Quinn, D. M. *Biochim. Biophys. Acta* **1990**, *1040*, 199-205.